Elastic electron scattering by excited hydrogen atoms in a laser field

Aurelia Cionga,[1] Fritz Ehlotzky,[2,*] and Gabriela Zloh[1]
[1]*Institute for Space Science, P.O. Box MG-23, R-76900 Bucharest, Romania*
[2]*Institute for Theoretical Physics, University of Innsbruck, Technikerstrasse 25, A-6020 Innsbruck, Austria*
(Received 29 March 2001; published 6 September 2001)

We consider electron scattering by hydrogen atoms in a linearly polarized laser field. The electrons may have sufficiently high energy in order that the scattering process can be treated in the first-order Born approximation. The scattered electrons, embedded in the laser field, are described by Gordon-Volkov waves. We assume that during the scattering, the hydrogen atoms are in an excited state (in particular, in the $2s$, $2p$, or $3s$ state) and that for moderate laser field intensities, it is sufficient to describe the interaction of the target atoms with the radiation field by first-order time-dependent perturbation theory. We discuss the angular dependence of the nonlinear differential scattering cross sections for low values N of emitted or absorbed laser photons, inspecting the contributions of the various electronic and atomic terms of the matrix elements. Detailed numerical results are presented for one-photon absorption at low-field intensities. We also compare our results with those obtained from the assumption of a static atomic polarizability, describing the laser dressing of the excited atomic states.

DOI: 10.1103/PhysRevA.64.043401 PACS number(s): 34.80.Qb, 34.50.Rk, 32.80.Wr

I. INTRODUCTION

The investigation of scattering of electrons by atoms in a laser field has by now a long history. Introductions into this field of research can be found in the books by Mittleman [1] and by Faisal [2]. A comprehensive survey on various aspects of this problem has been presented in our recent review [3]. As long as the laser frequencies are sufficiently low, the laser dressing of the atomic targets can be neglected and the atoms can be described by a structureless potential. This approximation was used in the seminal work of Bunkin and Fedorov [4] and of Kroll and Watson [5]. Investigations of laser-assisted electron scattering on a potential beyond the first-order Born approximation were done by Han [6]. Since now, various laser sources of higher frequencies have become available, the interaction of the laser radiation with the atomic electrons during the scattering process has become of relevance. As long as the laser fields are of moderate power, this laser dressing of the atomic target can be described by the time-dependent perturbation theory (TDPT). The investigation of free-free transitions during the scattering of electrons, mainly by hydrogen atoms in their ground state, has been considered by several authors, starting with the work of Gersten and Mittleman [7], Mittleman [8], and Zon [9]. The importance of laser-target interaction during electron-atom scattering in a laser field was discussed quite a number of years ago in two papers by Lami and Rahman [10,11]. These authors showed by treating the interaction with the laser field in the lowest order of TDPT, that for single-photon inverse bremsstrahlung the laser-target interaction begins to dominate over the laser-electron interaction for photon energies above about 4 eV. The most detailed investigations of our present topic were, however, those of Francken and Joachain and co-workers [12,13]. Further work on free-free transitions, including the laser-dressing of the atomic target in its ground state, was performed by Kracke *et al.* [14], Dörr *et al.* [15], and Cionga *et al.* [16,17]. Various approximation schemes were discussed in the work of Gavrila [18], Faisal [19,20], and Maquet *et al.* [21], and we refer to their work for further details. A summary of the experimental situation in the field of electron-atom scattering in a laser field can be found in the review by Mason [22].

To our knowledge, the above scattering process has been investigated in less detail for the case where the target atom is in an excited state. By intuitive reasoning, we may expect that with increasing excitation of the atomic system, the laser-dressing effects should become of increasing importance, in particular, at small scattering angles. Calculations on the scattering of electrons by hydrogen in its metastable $2s$ state were performed by Vučić and Hewitt [23]. Related investigations were recently presented by Purohit *et al.* [24] for resonant frequencies and by Korol' *et al.* [25].

In the present paper, we shall consider the scattering of electrons of higher kinetic energies of at least 100 eV by hydrogen atoms in excited states in the presence of a linearly polarized laser field of moderate power of some 10^{12} Wcm^{-2} such that target dressing can be treated by TDPT. Different frequencies of the laser field will be considered and we shall discuss the angular distribution of the differential cross sections (DCS) of the scattered electrons for the following two configurations of scattering, namely $\vec{\varepsilon}||\vec{k}_i$ and $\vec{\varepsilon}||\vec{q}$ where $\vec{k}_{i(f)}$ is the momentum of the ingoing (outgoing) electron, $\vec{q}=\vec{k}_i-\vec{k}_f$, the momentum transfer of scattering electron, and $\vec{\varepsilon}$ the unit vector of the linear polarization of the laser field. We shall devote particular attention to the contributions of the different parts of the matrix elements to the final values of the cross sections as a function of the

*Corresponding author.
Email address: Fritz.Ehlotzky@uibk.ac.at

scattering angle and compare our results with those obtained, if the target dressing is described by a laser-induced polarization potential with a static polarizability.

Section II will be devoted to the presentation of the theoretical basis of our calculations. In Sec. III, we shall discuss a number of representative numerical examples for the hydrogen atom in its $2s$, $2p$, and $3s$ state. While the first state is metastable, and therefore, the presented data will be accessible to observation, the second and third case will be considered to discuss the effect of target dressing as a function of the excitation of the atom. Finally, in Sec. IV, we shall summarize our results and make some concluding remarks. Atomic units will be used throughout this paper.

II. BASIC THEORY FOR MODERATE INTENSITIES

We assume that for moderate laser field intensities we can treat the field-atom interaction by TDPT [26]. We shall use first-order TDPT to describe the excited states of hydrogen embedded in a laser field. Based on the work of Florescu *et al.* [27], we can write down an approximate solution for an electron bound to a Coulomb potential in the presence of a monochromatic electromagnetic plane wave as follows:

$$|\Psi_{nlm}(t)\rangle = e^{-i\mathrm{E}_n t}[|\psi_{nlm}\rangle + |\psi^{(1)}_{nlm}\rangle], \tag{1}$$

where $|\psi_{nlm}\rangle$ is an unperturbed excited state of hydrogen of energy E_n and $|\psi^{(1)}_{nlm}\rangle$ denotes the related first-order radiative correction. According to Florescu and Marian [28], this correction can be written in terms of the linear response, defined by

$$|\vec{w}_{nlm}(\Omega)\rangle = -G_C(\Omega)\vec{P}|\psi_{nlm}\rangle. \tag{2}$$

Here, $G_C(\Omega)$ is the Coulomb Green function and $\vec{P}$ is the momentum operator of the bound electron. Two values of the argument of the Green functions are necessary in order to write down the approximate solution Eq. (1), namely,

$$\Omega^{\pm} = \mathrm{E}_n \pm \omega. \tag{3}$$

As in the formalism developed by Byron and Joachain [26], we describe the initial and final states of the scattered electron by Gordon-Volkov waves. For an electron of kinetic energy E_k and momentum $\vec{k}$, the corresponding solution reads

$$\chi_{\vec{k}}(\vec{r},t) = \frac{1}{(2\pi)^{3/2}}\exp\{-iE_k t + i\vec{k}\cdot\vec{r} - i\vec{k}\cdot\vec{\alpha}(t)\}, \tag{4}$$

where $\vec{\alpha}(t)$ describes the classical oscillation of the electron in the electric field $\vec{\mathcal{E}}(t)$ of the plane wave in dipole approximation, namely,

$$\vec{\alpha}(t) = \alpha_0\vec{\varepsilon}\sin\omega t. \tag{5}$$

Here, $\alpha_0 = \mathcal{E}_0/\omega^2$ with the field amplitude $\mathcal{E}_0$ and the laser frequency ω. In Eq. (4), the A^2 part of the electromagnetic interaction has been dropped since it does not contribute in dipole approximation to scattering processes.

We restrict our considerations to high scattering energies for which the first-order Born approximation in terms of the scattering potential is sufficiently accurate. Neglecting exchange effects, we describe the electron-atom interaction by the static potential

$$V(r,R) = -\frac{1}{r} + \frac{1}{|\vec{r}-\vec{R}|}. \tag{6}$$

Then, the S-matrix element of elastic electron-atom scattering is given by

$$S^{B1}_{if} = -i\int_{-\infty}^{+\infty} dt\langle\chi_{\vec{k}_f}(t)\Psi_{nlm}(t)|V(r,R)|\chi_{\vec{k}_i}(t)\Psi_{nlm}(t)\rangle, \tag{7}$$

where Ψ_{nlm} and $\chi_{\vec{k}_{i(f)}}$ are given by Eqs. (1) and (4), respectively. As we concentrate on free-free transitions, the initial and final atomic states will be identical.

In the presence of the radiation field, the scattered electron can gain or lose energy such that $E_f = E_i + N\omega$, where $E_{i(f)}$ is the initial (final) kinetic energy of the electron. N is the net number of photons exchanged (absorbed or emitted) by the colliding system and the laser field. Therefore, the energy spectrum of the scattered electrons consists of the elastic term with $N=0$ and of a number of sidebands. Each pair of sidebands has the same value of $|N|$.

The DCS for a process in which N photons are involved can be expressed by

$$\frac{d\sigma_N}{d\Omega} = (2\pi)^4\frac{k_f(N)}{k_i}|T_N|^2, \tag{8}$$

where the transition matrix element, evaluated from the S matrix element Eq. (7), has the following general structure:

$$T_N = T_N^{(0)} + T_N^{(1)}. \tag{9}$$

The first term is given by

$$T_N^{(0)} = J_N(\vec{\alpha}_0\cdot\vec{q})\langle\psi_{nlm}|F(\vec{q})|\psi_{nlm}\rangle, \tag{10}$$

and is related to the Bunkin-Fedorov formula [4], in which the laser dressing of the target is neglected. In this case, T_N reduces to $T_N^{(0)}$ and the ordinary Bessel function $J_N(\vec{\alpha}_0\cdot\vec{q})$ contains all the field dependences of the transition matrix element. $F(\vec{q})$ is the operator of the form factor and reads

$$F(\vec{q}) = \frac{1}{2\pi^2 q^2}[\exp(i\vec{q}\cdot\vec{r}) - 1], \tag{11}$$

with $\vec{q}=\vec{k}_i-\vec{k}_f$.

The second term on the right-hand side of Eq. (9) describes the first-order radiative correction to the atomic state. Here, one of the N photons exchanged between the field and the colliding system interacts with the bound electron. This photon can be emitted or absorbed while the other $N\pm1$ photons interact with the scattered electron. After the integration over the coordinates of the scattered electron has been performed, the general structure of $T_N^{(1)}$ is given by

$$T_N^{(1)}=-\frac{\alpha_0\omega}{2}[J_{N-1}(\vec{\alpha}_0\cdot\vec{q})\mathcal{M}_{at}^{(I)}(\Omega^+) + J_{N+1}(\vec{\alpha}_0\cdot\vec{q})\mathcal{M}_{at}^{(I)}(\Omega^-)]. \tag{12}$$

The transition matrix elements $\mathcal{M}_{at}^{(I)}(\Omega^\pm)$ refer to the exchange of one photon between the atomic electron and the field. In terms of the linear response Eq. (2), the corresponding expression reads in the case of absorption

$$\mathcal{M}_{at}^{(I)}(\Omega^+)=\langle\psi_{nlm}|F(\vec{q})|\vec{\varepsilon}\cdot\vec{w}_{nlm}(\Omega^+)\rangle + \langle\vec{\varepsilon}^*\cdot\vec{w}_{nlm}(\Omega^-)|F(\vec{q})|\psi_{nlm}\rangle \tag{13}$$

and for emission

$$\mathcal{M}_{at}^{(I)}(\Omega^-)=\langle\psi_{nlm}|F(\vec{q})|\vec{\varepsilon}^*\cdot\vec{w}_{nlm}(\Omega^-)\rangle + \langle\vec{\varepsilon}\cdot\vec{w}_{nlm}(\Omega^+)|F(\vec{q})|\psi_{nlm}\rangle, \tag{14}$$

respectively.

A. Scattering by hydrogen in the 2s state

For the $2s$ state, the atomic matrix element appearing in Eq. (10) reads

$$\langle\psi_{2s}|F(\vec{q})|\psi_{2s}\rangle=-\frac{1}{2\pi^2}\frac{q^6+4q^4+4q^2+7}{(q^2+1)^4}\equiv-\frac{1}{(2\pi)^2}f_{el}^{B1}, \tag{15}$$

where f_{el}^{B1} is the first-order Born approximation for the transition amplitude of elastic electron scattering by a hydrogen atom in its $2s$ state.

For the evaluation of the matrix elements Eqs. (13) and (14) the expression for the linear response Eq. (2) used was evaluated by Florescu and Marian [28] [see Eqs. (9) and (28) in this work]. After the angular integrations have been performed, we obtain

$$\mathcal{M}_{at}^{(I)}(\Omega^+)=-\frac{\vec{\varepsilon}\cdot\vec{q}}{2\pi^2q^3}\tilde{\mathcal{J}}_{201}^a(\omega,q),$$

$$\mathcal{M}_{at}^{(I)}(\Omega^-)=\frac{\vec{\varepsilon}^*\cdot\vec{q}}{2\pi^2q^3}\tilde{\mathcal{J}}_{201}^a(\omega,q). \tag{16}$$

We were able to derive an analytic expression for $\tilde{\mathcal{J}}_{201}^a(\omega,q)$ in terms of hypergeometric functions. The details are presented in Appendix A. By means of the expressions in Eq. (16), we can write down the following explicit formula for $T_N^{(1)}$ in the case of linear laser polarization:

$$T_N^{(1)}=\frac{\alpha_0\omega}{2\pi^2q^2}\frac{\vec{\varepsilon}\cdot\vec{q}}{q}J_N'(\vec{\alpha}_0\cdot\vec{q})\tilde{\mathcal{J}}_{201}^a(\omega,q), \tag{17}$$

where $J_N'(\vec{\alpha}_0\cdot\vec{q})$ is the first derivative of the Bessel function with respect to its argument. It satisfies the well-known relation

$$J_N'(\vec{\alpha}_0\cdot\vec{q})=\frac{1}{2}[J_{N-1}(\vec{\alpha}_0\cdot\vec{q})-J_{N+1}(\vec{\alpha}_0\cdot\vec{q})]. \tag{18}$$

Within the framework of the above approximation, in which the first-order radiative correction to the $2s$ state is taken into account only, the DCS for a process in which N photons are exchanged between the colliding system and a linearly polarized laser field is given by

$$\frac{d\sigma_N}{d\Omega}=\frac{k_f}{k_i}\left|f_{el}^{B1}(q)J_N(\vec{\alpha}_0\cdot\vec{q}) - 2\alpha_0\omega\frac{\vec{\varepsilon}\cdot\vec{q}}{q^3}J_N'(\vec{\alpha}_0\cdot\vec{q})\tilde{\mathcal{J}}_{201}^a(\omega,q)\right|^2. \tag{19}$$

Taking the low-frequency limit of $\tilde{\mathcal{J}}_{201}^a(\omega,q)$, we can show that the expression for the DCS in Eq. (19) takes the form

$$\frac{d\sigma_N}{d\Omega}\simeq\frac{k_f}{k_i}\left|f_{el}^{B1}(q)J_N(\vec{\alpha}_0\cdot\vec{q}) - 24\frac{10-61q^2+24q^4+15q^6}{(q^2+1)^6}\mathcal{E}_0\frac{\vec{\varepsilon}\cdot\vec{q}}{q^2}J_N'(\vec{\alpha}_0\cdot\vec{q})\right|^2 \tag{20}$$

and it is worthwhile to compare this expression with Eq. (2.31a) in the work of Byron *et al.* [30] and Eq. (1) in the paper of Zon [9], evaluated for the $1s$ state. Moreover, for small scattering angles, and hence, for $q\ll1$, the factor in front of $\mathcal{E}_0$ in Eq. (20) can be approximated by the numerical value 240 a.u.$\simeq2\alpha_{2s}$, where α_{2s} is the static polarizability of the $2s$ state. Its value is much larger than the polarizability of the ground state, $\alpha_{1s}=4.5$ a.u.. In general, we learn from the tables of Radzig and Smirnov [29] that the dipole polarizability of the subshell nl of the hydrogen atom is given by

$$\alpha_{nl}=n^6+\frac{7}{4}n^4(l^2+l+2). \tag{21}$$

We therefore expect stronger dressing effects for excited states, and consequently, an increased probability for their experimental verification.

For weak laser fields at any scattering angle and for moderate laser intensities at small scattering angles, i.e., whenever the arguments of the Bessel functions are small, the

following DCS expression can be derived from Eq. (19) for the absorption of one photon ($N=1$):

$$\frac{d\sigma_1}{d\Omega} \simeq \frac{(\vec{\alpha}_0\cdot\vec{q})^2}{4}\frac{k_f}{k_i}\left| f_{el}^{B1} - 2\frac{\omega}{q^3}\tilde{\mathcal{J}}^a_{201}(\omega,q)\right|^2 \tag{22}$$

and a similar expression can be found for $N=-1$, describing one-photon emission in the perturbative regime.

B. Scattering by hydrogen in the 2*p* states

The elastic scattering of electrons by laser-dressed hydrogen atoms in the $2p$ states can be treated in a similar manner. Here, the form-factor matrix element $\langle\psi_{2pm}|F(\vec{q})|\psi_{2pm}\rangle$, appearing in $T_N^{(0)}$, can be evaluated from the formula

$$\langle\psi_{2pm}|\exp(i\vec{q}\cdot\vec{r})|\psi_{2pm}\rangle = -\frac{1}{(q^2+1)^4}\left\{(q^2-1) - 4\sqrt{\frac{\pi}{5}}q^2(3m^2-2)Y_{20}(\hat{q})\right\}. \tag{23}$$

On the other hand, the matrix element $T_N^{(1)}$ of Eq. (12) reads after the angular integration was performed

$$T_N^{(1)} = \frac{\alpha_0\omega}{2\pi^2 q^2}\frac{\vec{\varepsilon}\cdot\vec{q}}{q}J'_N(\vec{\alpha}_0\cdot\vec{q})\left[\tilde{\mathcal{J}}^c_{210}(\omega,q)\,\delta_{m0} + \frac{1}{5}(4-m^2)\tilde{\mathcal{J}}^c_{212}(\omega,q)\right]. \tag{24}$$

We want to have the analytic expression in the above formula as simple as possible for all future calculations. We therefore consider $\vec{\varepsilon}$ to define the quantization axes. For that case, the explicit analytic expressions for the two new radial integrals appearing in Eqs. (23,24) are presented in Appendix B.

In order to be able to trace the relationship between the laser-induced dressing effects and the static atomic polarizability of the $2p$ state, we evaluated $\tilde{\mathcal{J}}^c_{21l'}$, defined in Eqs. (B1) of Appendix B, in the low frequency limit. This leads to the expressions

$$\tilde{\mathcal{J}}^c_{210}(\omega,q) \simeq 4q\omega\frac{2-57q^2+24q^4+3q^6}{(q^2+1)^6}, \tag{25}$$

$$\tilde{\mathcal{J}}^c_{212}(\omega,q) \simeq 4q\omega\frac{65-30q^2-15q^4}{(q^2+1)^6}. \tag{26}$$

If we moreover take $q \ll 1$ a.u., then we find

$$\tilde{\mathcal{J}}^c_{210}(\omega,q) \simeq 8q\omega \quad \text{and} \quad \tilde{\mathcal{J}}^c_{212}(\omega,q) \simeq 260q\omega. \tag{27}$$

Consequently, we obtain after summation over the magnetic quantum number m the following expression for the matrix element Eq. (9) in the low-frequency limit and for small momentum transfer:

$$T_N \simeq \frac{3}{(2\pi)^2}\left\{\frac{2}{q^2}\left[\frac{q^2-1}{(q^2+1)^4}+1\right]J_N(\vec{\alpha}_0\cdot\vec{q}) - 2\alpha_{2p}\mathcal{E}_0\frac{\vec{\varepsilon}\cdot\vec{q}}{q^2}J'_N(\vec{\alpha}_0\cdot\vec{q})\right\}. \tag{28}$$

This is the transition matrix element of laser-assisted elastic electron scattering by hydrogen in its $2p$ states at low-photon energies ω and small values of the momentum transfer $\vec{q}$. α_{2p} denotes the static polarizability of the $2p$ subshell. Its value, $\alpha_{2p}=176$ a.u., evaluatet from Eq. (21), exceeds by almost 50% the value of α_{2s} for the $2s$ state.

C. Scattering by hydrogen in the 3*s* state

We shall also devote some attention to the study of the $3s$ states since, according to the general expression Eq. (21), its static polarizability is even higher ($\alpha_{3s}=1012.5$ a.u.) than those of the first two excited subshells, discussed before. The formalism, presented in the previous section A for the $2s$ state, can be extended to lead in the present case to the following DCS formula:

$$\frac{d\sigma_N}{d\Omega} = \frac{k_f}{k_i}\left| f_{el}^{B1}(q)J_N(\vec{\alpha}_0\cdot\vec{q}) - 2\alpha_0\omega\frac{\vec{\varepsilon}\cdot\vec{q}}{q^3}J'_N(\vec{\alpha}_0\cdot\vec{q})\tilde{\mathcal{J}}^a_{301}(\omega,q)\right|^2. \tag{29}$$

The evaluation of the field free-scattering amplitude f_{el}^{B1} in the first-order Born approximation yields, in the present case,

$$f_{el}^{B1} \equiv -(2\pi)^2\langle\psi_{3s}|F(\vec{q})|\psi_{3s}\rangle = -\frac{2}{q^2}[\mathcal{I}_{30}(q)-1], \tag{30}$$

where the relevant expression for the radial integral $\mathcal{I}_{30}(q)$ can be derived from the general formula Eq. (A13), whereas the appropriate structure of the term $\tilde{\mathcal{J}}^a_{301}(\omega,q)$ in Eq. (29) can be inferred from Eq. (A9) of Appendix A.

The straightforward generalization of the above formalism to free-free transitions by hydrogen in any ns state is possible, if we use the relevant expressions for f_{el}^{B1}, $\mathcal{I}_{n0}(q)$, and $\tilde{\mathcal{J}}^a_{n01}(\omega,q)$. The general form of the two radial integrals $\mathcal{I}_{n0}(q)$ and $\tilde{\mathcal{J}}^a_{n01}(\omega,q)$ have been explicitly written down in Appendix A.

III. NUMERICAL RESULTS AND DISCUSSION

In our presentation of numerical examples, we shall first concentrate on the study of free-free transitions by a hydrogen atom in its metastable $2s$ state. Since this state has a sufficiently long lifetime, the presented effects should be ac-

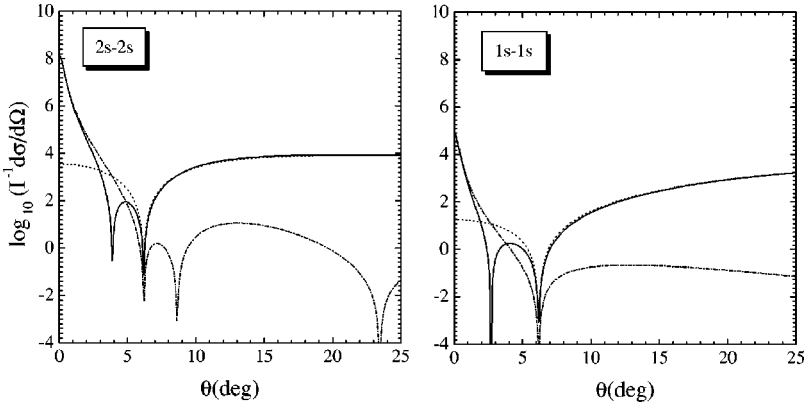

FIG. 1. Shows the DCS data, normalized with respect to the field intensity and with $\vec{\varepsilon}||\vec{k}_i$, for scattering by hydrogen and for the parameter values $N=1$, $E_i=100$ eV, $\omega=1.17$ eV. In the left panel, hydrogen is in its $2s$ state and for comparison, in the right panel are the corresponding data for the $1s$ state. The increase of the dressing effects below the kinematical minimum at $\theta=6°$ is remarkably large. Actually, the electronic as well as the atomic effects are increasing by going to the metastable excited state.

cessible to observation. We consider the scattering of electrons of initial kinetic energy $E_i=100$ eV, for the kinematic geometry in which the initial momentum $\vec{k}_i$ of the electron points parallel to the vector $\vec{\varepsilon}$ of linear polarization. The common direction of these vectors will define the z axis. All calculations presented below were made for moderate laser field intensities such that $I \leqslant 3.5\times 10^{10}$ Wcm^{-2}.

We shall first demonstrate that at small scattering angles, where the dressing effects are important, the laser-assisted scattering signals are significantly stronger for hydrogen in the $2s$ state in comparison with the data for the $1s$ state. This finding is intuitively understandable, if we remember our previous remark, using Eq. (21), about the relationship between the dressing effects and the static polarizabilities of the hydrogenic states, namely $\alpha_{2s}=120$ a.u. and $\alpha_{1s}=4.5$ a.u.

In Fig. 1, we plotted the DCS (normalized with respect to the laser intensity) for one-photon absorption ($N=1$). We used the frequency $\omega=1.17$ eV of a Nd:YAG laser and we present the free-free transition data for the $2s$ state in panel (a) and for the $1s$ state in panel (b). Full lines are used to show the DCS, evaluated by including the dressing of the target and dotted lines refer to the corresponding data obtained from the Bunkin-Fedorov low-frequency approximation Eq. (10). The dash-dotted curves are used to present the dressing contributions of $(2\pi)^4(k_f/k_i)|T_1^{(1)}|^2$ to the DCS only. We immediately see that at small scattering angles, the laser-assisted signals are by roughly three orders of magnitude stronger for the $2s$ than for the $1s$ state. We also note that in this scattering geometry, all curves shown have a minimum at $\theta=\arccos(k_i/k_f)$. In laser-assisted elastic electron-atom scattering, this angle does not depend on the particular state of the atomic target but only on the energy of the scattered electron and on the laser frequency. Therefore, it has the same value in panels (a) and (b) at approximately $\theta=6°$. Moreover, the DCS have another minimum caused by the interference between the electronic and the atomic contributions. This minimum, however, depends on the target state considered. We shall present some further considerations on these interference minima in a paragraph further below.

In Fig. 2, we show the DCS for a different frequency, namely, $\omega=2$ eV of a He:Ne laser. Some of the comments made about the data of the foregoing Fig. 1 remain also true in the present case. Again, the laser-assisted signals are significantly stronger for hydrogen in the $2s$ state if compared with the data for the $1s$ state, namely almost four orders of magnitude in the forward direction. Similarly, the kinematical minimum has the same position for the $2s$ and the $1s$ states. Here, however, it is located at $\theta=8°$, which is different from the value in Fig. 1. Moreover, we stress the different character of the interferences between the electronic and atomic contributions for the excited state and for the ground state, respectively. These interferences are constructive for the $2s$ state, but they are destructive for the $1s$ state.

For a better understanding of this changing behavior, we present in Fig. 3, the frequency dependence of the DCS as a full line, as well as the separate frequency behavior of the electronic (dotted line) and of the atomic (chain line) term, respectively. We used the same geometry and the same initial

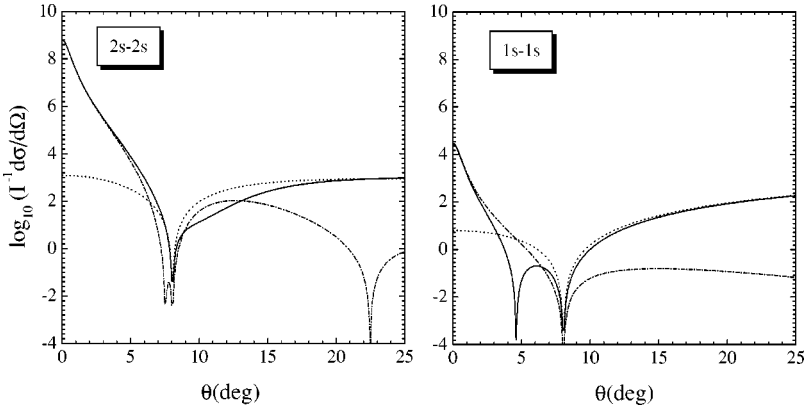

FIG. 2. Presents similar data for the same parameters as in Fig. 1, except for the higher laser frequency $\omega=2$ eV. The kinematical minimum is now at $\theta=8°$ and the dressing effects have increased further, if compared with the results of Fig. 1, for the $1s$, as well as for the $2s$ state.

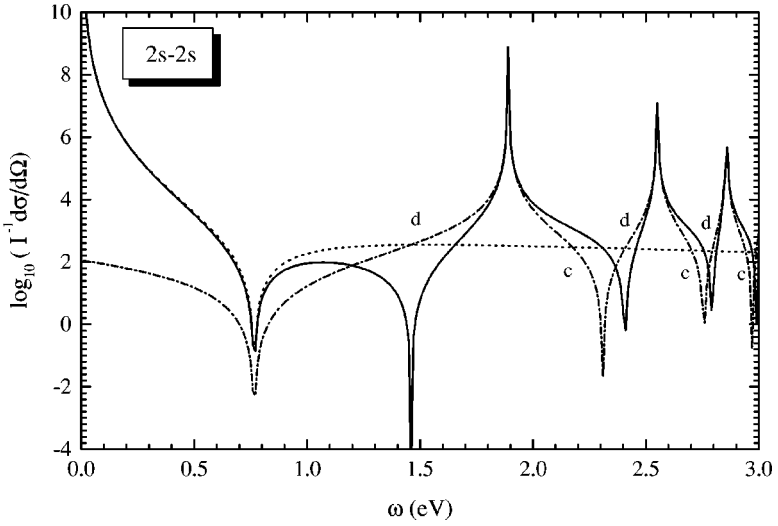

FIG. 3. Discusses for the same configuration as before the frequency dependence of the DCS for $N=1$ at the fixed scattering angle $\theta=5°$, if the hydrogen target is in the $2s$ state. While the data, evaluated from the electronic term (as a dotted line), show a rather smooth behavior, the results of the atomic contribution (as a dash-dotted line) are passing through various resonances with increasing frequency, yielding constructive and destructive interferences with the electronic term. For $\omega\rightarrow 0$, target dressing becomes a negligible effect.

energy of the scattered electron as in the previous two figures. The scattering angle was chosen to be $\theta=5°$. We immediately recognize that the chosen laser frequency $\omega=2$ eV is close to the atomic resonance $2s-3p$. Hence, whenever a crossing of an atomic resonance takes place, the atomic term will change its sign, and thus, the character of the interferences will change, as can be seen at the points denoted by *c* and by *d*, respectively. The data of this figure also indicate that laser dressing of the atomic states becomes negligible for small radiation frequencies.

It is quite useful to discuss under what circumstances we can safely use the closure approximation or, alternatively, the low-frequency approximation to describe the laser dressing of the target atom. For that purpose we plotted in Fig. 4 the atomic contribution, given by $(2\pi)^4(k_f/k_i)|T_1^{(1)}|^2$, to the DCS. $T_1^{(1)}$ was evaluated from Eq. (12) for small arguments of the Bessel functions using for comparison of the data: (i) the explicit first-order dressing calculation, adopted here (shown as the dash-dotted line), (ii) the low-frequency limit of this calculation (dashed line), or (iii) the corresponding closure approximation (dotted line). We conclude from these respective data that the two latter approximations work quite well at very small scattering angles and for laser frequencies that are sufficiently far away from any resonances, as we can quite clearly see by considering the data in the left panel for $\omega=1.17$ eV. At larger scattering angles, however, the closure approximation is no longer a useful approximation, since it is unable to describe the known decrease of the dressing effects. An improvement of the closure approximation, suggested by Milošević *et al.* [31], consists in replacing the static polarizability α_s by the so-called dynamic polarizability $\alpha_d(\vec{q})=2/\bar{E}(1+q^2/4)^3$ where $\bar{E}\simeq 4/9$ a.u.. But, whenever the laser frequency ω matches an atomic resonance, neither the low-frequency limit is useful nor the closure approximation can be appropriately applied. This situation is demonstrated for $\omega=2$ eV by the data shown in the right panel of Fig. 4. Here, neither of the two approximations can describe the dressing effects fairly well.

In the following, we shall compare the numerical data obtained from our present theoretical anlysis with those results that were evaluated by means of another approach to the investigation of the same problem, using different methods.

We begin by showing in Fig. 5, using full lines, the DCS for a different initial electron energy of $E_i=500$ eV and for a different scattering geometry where the unit vector of laser polarization $\vec{\varepsilon}$ is taken parallel to the momentum transfer $\vec{q}$ such that no kinematical minimum exists. For the data presented, we used four laser frequencies, namely, $\omega=2.33$, 2, 1.165, and 0.825 eV. The quantum- interference between the electronic contribution (dotted line) and the atomic part

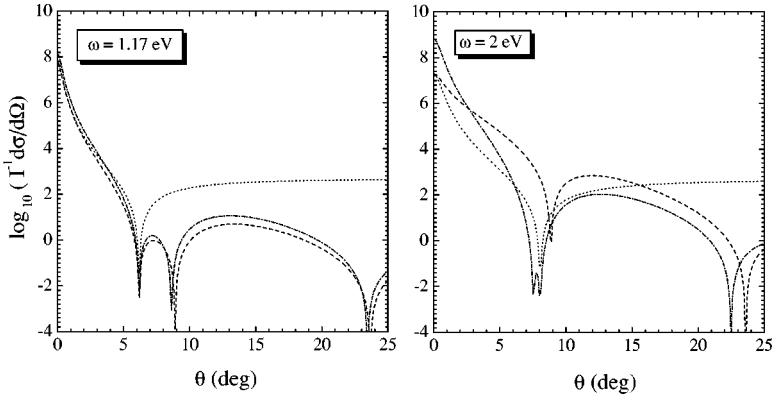

FIG. 4. Shows a comparison between the results for the atomic contribution $(2\pi)^4(k_f/k_i)|T_1^{(1)}|^2$ evaluated by using (i) the first-order dressing calculation, adopted here (dash-dotted line), (ii) the corresponding low-frequency limit (dashed line), or (iii) the closure approximation (dotted line). $\omega=1.17$ eV in the left panel and $\omega=2$ eV in the right one. The electron energy is $E_i=100$ eV and the kinematic choice is $\vec{\varepsilon}||\vec{k}_i$.

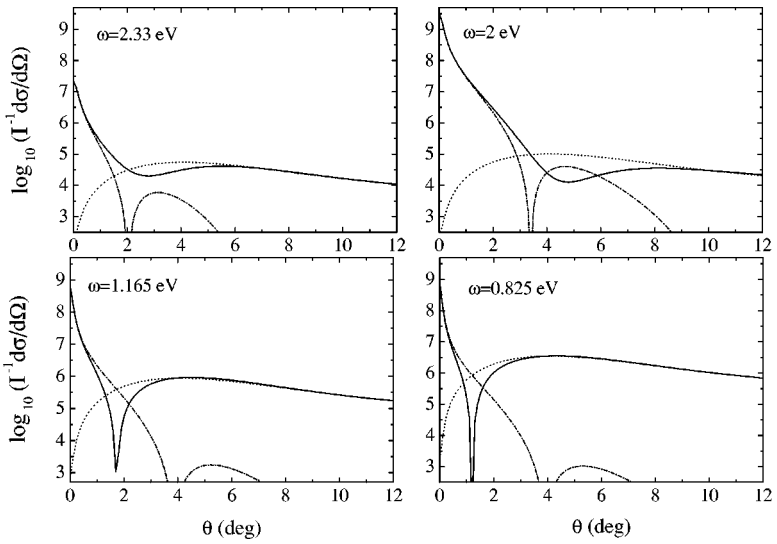

FIG. 5. Discusses for hydrogen in the $2s$ state and the higher electron energy $E_i=500$ eV the θ dependence of the DCS with increasing laser frequencies. Depending on the constructive or destructive interferences of the electronic (dotted) and atomic (dash-dotted) term, the final appearance of dressing effects will be enhanced or suppressed. In all panels we have $\vec{\varepsilon}||\vec{q}$.

(dash-dotted line) is apparently destructive for the lower-two frequencies ($\omega=0.825$ and 1.165 eV), leading to deep minima at $\theta\simeq 1°$ and 2°, respectively. The behavior of the DCS for the other two frequencies is quite different. For example, at $\omega=2$ eV there is a constructive interferences at $\theta=3°$. This is followed by a destructive interference leading to a minimum near $\theta=5°$. The change in the interference character is the result of a change in the sign of the atomic contribution (determined by the matrix element $T_1^{(1)}$), at $\theta\simeq 3.5°$. The data for the DCS, shown in the panels of this figure as a full line, are in quantitative agreement with those results presented by Vučić and Hewitt [23] in their Fig. 1. These authors used the Born-Floquet theory to evaluate the DCS at the laser intensity $I=1.327\times 10^9$ Wcm^{-2}. Our present comparison confirms that the method employed by the above authors and our approach are comparable in their results at moderate laser intensities, as long as our perturbative treatment includes the appropriate number of terms.

Next, we inspect the explicit expression for $\mathcal{J}^a_{201}(\tau,q)$ in Eq. (A4) of Appendix A. Here, the radial integral $\mathcal{J}^a_{201}(\Omega^+,q)$ has poles for $\tau^+=n$ with $n\geqslant 3$. These poles are related to the resonances seen in our Fig. 3 and correspond to frequencies which match the $2s-np$ atomic transitions. We conclude that our formalism permits to treat resonance effects in laser-assisted electron-atom scattering that go beyond the two-level approximation of the atomic system and does not require the use of the rotating-wave approximation, as considered by Purohit *et al.* [24]. Our formulation of the problem is much more general, being suitable for the application of linearly, as well as circularly, polarized laser light.

If we look at the radial probability distributions of hydrogen for its lowest levels, presented in the book by Condon and Shortley [33], we immediately realize that the $2p$ and $3s$ states should have even higher static polarizabilities than the $1s$ and $2s$ states considered before. These polarizabilities can indeed be calculated from the general formula (21) to be $\alpha_{2p}=176$ a.u. and $\alpha_{3s}=1012.5$ a.u.. We therefore expect that laser dressing in electron scattering by hydrogen in the $2p$ and $3s$ states will be even more important. Although these states rapidly decay by dipole transitions, we nevertheless thought it worthwhile to present the corresponding scattering data for comparison with the foregoing findings. The considered scattering geometry, initial electron energy, and laser intensity will be the same as in Figs. 1–4.

In Fig. 6, we show the DCS data for $N=1$ in the panels (a) and (b) for electron scattering by hydrogen in the $2p$ state and in the panels (c) and (d) for scattering by hydrogen in the $3s$ state. In panel (a), we took the laser frequency $\omega=1.17$ eV and in panel (b) we chose $\omega=2$ eV. The kinematical minimum is at $\theta=6°$ in the left panel and at $\theta=8°$ in the right panel. The DCS, including the atomic laser dressing, are drawn as full lines, the Bunkin-Fedorov data, evaluated from the static atomic potential (6), are presented as dotted lines, and the purely atomic part $(2\pi)^4(k_f/k_i)|T_1^{(1)}|^2$ is shown by dash-dotted lines. We recognize that below the kinematical minimum, the dressing effects have markedly increased, if compared with the data in Figs. 1 and 2 for hydrogen in the $2s$ state for $\omega=1.17$ and 2 eV, respectively. This is understandable since the static polarizability of the $2p$ state is larger by a factor 1.46 than the polarizability of the $2s$ state. For considering scattering by hydrogen in the $3s$ state, we took $\omega=0.117$ eV for the data in the panel (c) and $\omega=1.17$ eV for the results in the panel (d). As before, the full lines represent the DCS including the laser dressing and the dotted lines represent the Bunkin-Fedorov approximation. We also plotted the atomic contribution $(2\pi)^4(k_f/k_i)|T_1^{(1)}|^2$ shown by a dash-dotted line, and finally, the corresponding data in the closure approximation by a dashed line. As expected, the DCS have increased since $\alpha_{3s}=1012.5$ a.u. is almost one order of magnitude larger than $\alpha_{2s}=120$ a.u. In addition, the DCS for $\omega=0.117$ eV are still larger than those for $\omega=1.17$ eV. This can be explained by means of the λ^4-power law of the low-frequency theorem of Brown and Goble [34]. Although the closure approximation might be considered fair for forward scattering at $\omega=0.117$ eV, we find it interesting to note that it is quite inadequate for $\omega=1.17$ eV. We therefore call attention to the fact that a statement concerning the validity of the closure approximation at low frequency should be critically analyzed.

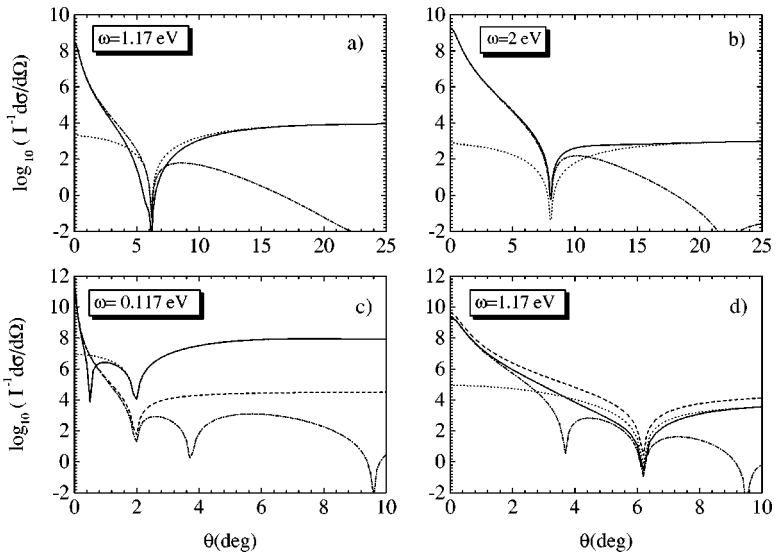

FIG. 6. Presents the DCS for the same configuration and initial energy E_i as in Figs. 1 and 2 but now for hydrogen in its $2p$ state in the panels (a) and (b), where we took $\omega=1.17$ eV in the left panel and $\omega=2$ eV in the right one. Moreover, panels (c) and (d) show finally the DCS for hydrogen in its $3s$ state. The laser frequency is $\omega=0.117$ eV in the left panel and $\omega=1.17$ eV in the right one. The full line represents the DCS, including laser dressing of the atom and the dotted line refers to the Bunkin-Fedorov approximation. We also plotted the atomic contribution $(2\pi)^4(k_f/k_i)|T_1^{(1)}|^2$ shown by a dash-dotted line and its results in the closure approximation, represented by a dashed line.

IV. SUMMARY AND CONCLUSIONS

In the present paper we investigated the scattering of fast electrons by hydrogen atoms in a laser field. It was assumed that during the scattering, the hydrogen atoms are not in their ground state but in one of the low-lying excited states. We included the laser dressing of these excited states by using TDPT in lowest order of the laser field strength and we described the scattered electron, embedded in the laser field, by the well-known Gordon-Volkov solution. Since we chose sufficiently high-electron energies, we were permitted to treat the scattering process within the frame work of the first-order Born approximation. For describing the laser-dressed excited atomic states we used a formalism, developed in earlier works [27,28]. This formalism can be used to describe in first-order TDPT the laser dressing of an arbitrary hydrogenic state and the corresponding radial integrals related to free-free transitions are presented in the two appendices. Our calculations show that also for the discussion of free-free transitions by excited states of the laser-dressed hydrogen atom, the closure approximation is a reasonable approximation below the kinematical minimum of the cross sections at $\theta=\arccos(k_i/k_f)$ and this approximation improves with decreasing laser frequency. On the other hand, the dressing effects increase with increasing excitation of the atomic system that is reflected by the increasing static polarizability α_s of these states. Moreover, for scattering angles beyond the kinematical minimum, the details of the atomic structure will, in general, become apparent in the scattering data evaluated by including all the details of the atomic and electronic contributions. We have compared our results for scattering by the metastable $2s$ state of hydrogen with similar calculations performed with Floquet methods and we found excellent agreement, showing the accuracy and efficiency of our method for moderate laser field intensities where TDPT is a reliable procedure to treat the laser dressing of the atomic states.

ACKNOWLEDGMENTS

This work was supported by a special research project for 2000/1 of the Austrian Ministry of Education, Science and Culture. We also acknowledge financial support by the University of Innsbruck under Reference No. 17011/68-00.

APPENDIX A

An analytic expression for $\tilde{\mathcal{J}}^a_{201}$ can be obtained by using the relation

$$\tilde{\mathcal{J}}^a_{201}(\omega,q)=\mathcal{J}^a_{201}(\Omega^+,q)-\mathcal{J}^a_{201}(\Omega^-,q), \tag{A1}$$

where the radial integral $\mathcal{J}^a_{201}(\Omega^\pm,q)$ is defined by

$$\mathcal{J}^a_{201}(\Omega^\pm,q)=\int_0^\infty dr r^2 R_{20}(r) j_1(qr) \mathcal{B}_{201}(\Omega^\pm;r), \tag{A2}$$

with $\mathcal{B}_{201}(\Omega^\pm;r)$ being presented in [28] by Eq. (33). $\mathcal{J}^a_{201}$ only depends on the photon frequency and on the magnitude of $\vec{q}$. The dependence on the frequency ω is determined through the parameters $\tau^\pm$, which are related to the parameters $\Omega^\pm$ defined in Eq. (3) by

$$\tau^\pm=1/\sqrt{-2\Omega^\pm}. \tag{A3}$$

Our result for $\mathcal{J}^a_{201}$ is shown below, expressed as a combination of nine Appell functions of two variables

$$\begin{aligned}\mathcal{J}^a_{201}(\tau,q)=&-\frac{\tau}{2^5 q^2}\left(\frac{4}{2+\tau}\right)^{3+\tau}\\ &\times\mathrm{Re}\Bigg\{4\chi_2^2[iS_1^a+(2q-i)\chi S_2^a-3q\chi^2 S_3^a]\\ &+\frac{(2+\tau)^2}{3-\tau}\chi_2^2[iS_1^b+(2q-i)\chi S_2^b-3q\chi^2 S_3^b]\\ &-\frac{8}{3-\tau}\chi_2^3\left[iS_1^c+\frac{3}{2}(2q-i)\chi S_2^c-6q\chi^2 S_3^c\right]\Bigg\}.\end{aligned} \tag{A4}$$

S_j^a, S_j^b, and S_j^c stand for

$$S_j^a = F_1(2-\tau,-2-\tau,1+j,3-\tau,\xi_2,\zeta_2),$$

$$S_j^b = F_1(3-\tau,-1-\tau,1+j,4-\tau,\xi_2,\zeta_2),$$

$$S_j^c = F_1(3-\tau,-2-\tau,2+j,4-\tau,\xi_2,\zeta_2), \tag{A5}$$

and we quote [32] for the definition of the function $F_1(a,b,b',c;x,y)$. The foregoing Eq. (A4) is written down for frequencies below the ionization threshold, where the parameters $\tau^{\pm}$ are real. The following additional notations are used

$$\chi_2 = \frac{2\tau}{\tau+2-2iq\tau}, \tag{A6}$$

$$\xi_2 = \frac{2-\tau}{4}, \quad \zeta_2 = \frac{2-\tau}{\tau+2-2iq\tau}. \tag{A7}$$

In the more general case, the radial integral reads

$$\mathcal{J}_{n01}^a(\tau^{\pm},q) = \int_0^{\infty} dr r^2 R_{n0}(r) j_1(qr) \mathcal{B}_{n01}(\Omega^{\pm};r) \tag{A8}$$

and appears in free-free transitions by hydrogen in any ns state. This leads with $\Omega^{\pm} = \mathrm{E}_n \pm \omega$ to

$$\begin{aligned}\mathcal{J}_{n01}^a(\tau,q) = &-\frac{1}{q}\frac{2^3\tau}{3(2-\tau)}\frac{1}{n^2(n-\tau)^2}\left(\frac{2n}{n+\tau}\right)^{\tau}\left(\frac{n-\tau}{n+\tau}\right)^{n} \\ &\times \mathrm{Re}\left\{\sum_{p=0}^{1}\frac{(1+p)!}{p!(1-p)!}\left(\frac{i}{2q}\right)^{p}\right. \\ &\times \sum_{k=-1,1} d_{n,0}^{1,-k}\left(\frac{n+\tau}{n-\tau}\right)^{k}\sum_{m=0}^{n-1}\frac{(1-n)_m}{m!(2)_m}\left(\frac{2}{n}\right)^{m} \\ &\times \sum_{\mu,\nu=0}^{\infty}\frac{1}{\mu!}\left[\frac{-(n+\tau)^2}{2n(n-\tau)}\right]^{\mu}\frac{1}{\nu!(4)_{\nu}}\left(\frac{4}{n-\tau}\right)^{\nu} \\ &\times (2-p+m+\nu)!\,\chi_n^{3-p+m+\nu}(2+k-n)_{\mu+\nu} \\ &\times \frac{(2-\tau)_{\mu+\nu}}{(3-\tau)_{\mu+\nu}} F_1(a,-n-\tau+1+k+\mu,3-p+m \\ &\left.+\nu,a+1,\xi_n,\zeta_n)\right\}. \end{aligned} \tag{A9}$$

The two variables of the Appell functions are then

$$\xi_n = \frac{n-\tau}{2n}, \quad \zeta_n = \frac{n-\tau}{n+\tau-iqn\tau}, \tag{A10}$$

and $d_{n,0}^{1,-k}$ is defined by Eq. (22) in [28]. $(n)_m$ denotes the Pochhammer's symbol and the following notations are used in addition:

$$\chi_n = \frac{n\tau}{n+\tau-iqn\tau}, \quad a = 2-\tau+\mu+\nu. \tag{A11}$$

The evaluation of the form-factor Eq. (11) requires the evaluation of the radial integral

$$\mathcal{I}_{n0}(\tau,q) = \int_0^{\infty} dr r^2 R_{n0}(r) j_0(qr) R_{n0}(r), \tag{A12}$$

and this is given by

$$\begin{aligned}\mathcal{I}_{n0}(\tau,q) &= \frac{1}{nq}\mathrm{Im}\left[\frac{n^2}{(2-iqn)^2}F_2\left(2,1-n,1-n,2,2,\right.\right. \\ &\qquad \left.\left.\frac{n}{2-iqn},\frac{n}{2-iqn}\right)\right] \\ &= 4\frac{(-1)^{n-1}}{n^3q^3}F_1\left(1-n,1-n,2,-\frac{4}{q^2n^2}\right) \\ &\quad \times \mathrm{Im}\left(\frac{qn}{2-iqn}\right)^{2n}. \end{aligned} \tag{A13}$$

APPENDIX B

In analogy to the case of the $2s$ state, the analytic expressions of the two radial integrals that appear in Eq. (24) for the $2p$ state are obtained by means of the relation

$$\tilde{\mathcal{J}}_{21l'}^c(\omega,q) = \mathcal{J}_{21l'}^c(\Omega^+,q) - \mathcal{J}_{21l'}^c(\Omega^-,q), \tag{B1}$$

where we have defined

$$\mathcal{J}_{21l'}^c(\Omega,q) = \int_0^{\infty} dr r^2 R_{21}(r) j_1(qr) \mathcal{B}_{21l'}(\Omega;r), \tag{B2}$$

with $l' = l \pm 1$. The functions $\mathcal{B}_{212}(\Omega;r)$ and $\mathcal{B}_{210}(\Omega;r)$ are presented in Eqs. (34,35) of [28]. In particular, $\mathcal{J}_{212}^c(\Omega,q)$ can be written down as a combination of two Appell functions, namely,

$$\mathcal{J}^c_{212}(\tau,q) = -\frac{\tau}{8q(3-\tau)}\left(\frac{4}{2+\tau}\right)^{3+\tau} \times \mathrm{Re}\left[\chi_2^4\left(4\chi_2 S^c_3 + \frac{i}{q}S^c_2\right)\right], \tag{B3}$$

while $\mathcal{J}^c_{210}(\Omega,q)$ is a combination of 10 Appell functions, viz.,

$$\mathcal{J}^c_{210}(\tau,q) = -\frac{\tau}{2^8 3q}\left(\frac{4}{2+\tau}\right)^{3+\tau}\mathrm{Re}\left\{\sum_{p=0}^{1}\frac{(1+p)!}{p!(1-p)!}\left(\frac{i}{2q}\right)^p \times \chi_2^{3-p}\left[-24\chi_2(3-p)!S^a_{3-p} - \frac{6(2+\tau)^2}{3-\tau}\chi_2(3-p)!S^b_{3-p} + \frac{16}{3-\tau}\chi_2^2(4-p)!S^c_{4-p} - \frac{48\tau}{1-\tau}\chi_2(2-p)!S^d_{2-p} + \frac{3\tau(2+\tau)^2}{3-\tau}(2-p)!S^e_{2-p}\right]\right\}. \tag{B4}$$

With reference to Eq. (A5), two additional notations were introduced here, namely,

$$S^d_j = F_1(1-\tau,-2-\tau,1+j,2-\tau,\xi_2,\zeta_2), \tag{B5}$$

$$S^e_j = F_1(3-\tau,-\tau,1+j,4-\tau,\xi_2,\zeta_2). \tag{B6}$$

[1] M. H. Mittleman, *Theory of Laser-Atom Interactions*, 2nd. ed. (Plenum, New York, 1993).
[2] F. H. M. Faisal, *Theory of Multiphoton Processes* (Plenum, New York, 1987).
[3] F. Ehlotzky, A. Jaroń, and J.Z. Kamiński, Phys. Rep. **297**, 63 (1998).
[4] F.V. Bunkin and M.V. Fedorov, Zh. Éksp. Teor. Fiz. **49**, 1215 (1965) [Sov. Phys. JETP **22**, 844 (1966)].
[5] N.M. Kroll and K.M. Watson, Phys. Rev. A **8**, 804 (1973).
[6] C.S. Han, Phys. Rev. A **51**, 4818 (1995).
[7] J.I. Gersten and M.H. Mittleman, Phys. Rev. A **13**, 123 (1976).
[8] M.H. Mittleman, Phys. Rev. A **18**, 685 (1978), and references quoted therein.
[9] B.A. Zon, Zh. Éksp. Teor. Fiz. **73**, 128 (1977) [Sov. Phys. JETP **46**, 65 (1977)].
[10] A. Lami and N.K. Rahman, J. Phys. B **14**, L523 (1981).
[11] A. Lami and N.K. Rahman, J. Phys. B **16**, L201 (1983).
[12] P. Francken and C.J. Joachain, J. Opt. Soc. Am. B **7**, 554 (1990), and references quoted therein.
[13] C.J. Joachain, M. Dörr, and N.J. Kylstra, Adv. At., Mol., Opt. Phys. **42**, 225 (1998).
[14] G. Kracke, J.S. Briggs, A. Dubois, A. Maquet, and V. Véniard, J. Phys. B **27**, 3241 (1994).
[15] M. Dörr, C.J. Joachain, R.M. Potvliege, and S. Vučić, Phys. Rev. A **49**, 4852 (1994).
[16] A. Cionga, F. Ehlotzky, and G. Zloh, Phys. Rev. A **61**, 063417 (2000).
[17] A. Cionga, F. Ehlotzky, and G. Zloh, Phys. Rev. A **62**, 063406 (2000).
[18] M. Gavrila, in *Collision Theory of Atoms and Molecules*, edited by F. A. Gianturco (Plenum, New York, 1989).
[19] F.H.M. Faisal, Comput. Phys. Rep. **9**, 55 (1989).
[20] F.H.M. Faisal, Radiat. Eff. Defects Solids **122-123**, 27 (1991).
[21] A. Maquet, V. Véniard, and T.A. Marian, J. Phys. B **31**, 3743 (1998).
[22] N.J. Mason, Rep. Prog. Phys. **56**, 1275 (1993).
[23] S. Vučić and R. Hewitt, Phys. Rev. A **56**, 4899 (1997).
[24] S.P. Purohit, A.K. Jain, and K.C. Mathur, Eur. Phys. J. D **2**, 41 (1998).
[25] A.V. Korol', O.I. Obolenskii, and A.V. Solov'ev, Tech. Phys. **44**, 1135 (1999).
[26] F.W. Byron, Jr. and C.J. Joachain, J. Phys. B **17**, L295 (1984).
[27] V. Florescu, A. Halasz, and M. Marinescu, Phys. Rev. A **47**, 394 (1993).
[28] V. Florescu and T. Marian, Phys. Rev. A **34**, 4641 (1986).
[29] A. A. Radzig and B. M Smirnov, *Reference Data on Atoms, Molecules, and Ions* (Springer, Berlin, 1985), p. 119.
[30] F.W. Byron, Jr., P. Franken, and C.J. Joachain, J. Phys. B **20**, 5487 (1987).
[31] D.B. Miloševi ć, F. Ehlotzky, and B. Piraux, J. Phys. B **30**, 4347 (1997).
[32] P. Appell and J. Kampé de Fériet, *Fonctions Hypergéométriques et Hypersphériques. Polynomes d'Hermite* (Gauthier-Villars, Paris, 1926).
[33] E. U. Condon and G. H. Shortley, *The Theory of Atomic Spectra* (University Press, Cambridge, 1953), p. 116.
[34] L.S. Brown and R.L. Goble, Phys. Rev. **173**, 1505 (1968).